Iraqi Journal of Physics, 2022 *Vol. 20, No. 1, PP. 82-92*
DOI: 10.30723/ijp.v20i1.973
P-ISSN: 2070-4003
E-ISSN: 2664-5548

Effect of Carbon Nanoparticles on the Performance Efficiency of a Solar Water Heater

Wasan L. Al-Salim [1a*], Jassim M. Al - Asadi [2b] and M. A. Mahdi [3c]
[1,2] Department of physics, College of Education for Pure Science, University of Basrah, Basrah, Iraq
[3] Department of Physics, College of Science, University of Basrah, Basrah, Iraq
[b]E-mail: Jassimalasadi10@gmail.com, [c]E-mail: m.a.mahdi@uobasrah.edu.iq
[a*]Corresponding author: wasanloay19@gmail.com

Abstract

Carbon nanoparticles are prepared by sonication using carbon black powder. The surface morphology of carbon black (CB) and carbon nanoparticles (CNPs) is investigated using scanning electron microscopy (SEM). The particles size ranges from 100 nm to 400 nm for CB and from 10 nm to 100 nm for CNPs. CNPs and CB are mixed with silicon glue of different ratios of 0.025, 0.2, 0.05, and 0.1 to synthesis films. The optical properties of the prepared films are investigated through reflectance and absorbance analyses. The ratio of 0.05 for CNPs and CB is the best for solar paint because of its higher solar water heater efficiency and is then added to the silicon glue. The temperature of cold water and temperature of hot water in the storage tank were tabulated on hourly basis with the help of an Arduino device. The atmospheric temperature was also noted. It was observed that the outlet temperature of the water was attained up to 75°C as compared to the inlet water temperature of 23°C for the tank applied with CNP-based paint. The tank applied with CNP-based paint has 4 °C higher water temperature than that coated with CB-based paint after 1 month of the test under sun irradiation. Based on the results, the efficiency of a solar water heater depends on the difference in temperature of inlet water and outlet of heater. The efficiency of the solar water heater coated with CNPs is around 77% but the solar water heater coated with CB has an efficiency of 67%.

Article Info.

Keywords:
Carbon nanoparticles, Solar water heaters, scanning electron microscopy, Optical properties, Thermal performance.

Article history:
Received: Jan. 16, 2022
Accepted: Feb. 24, 2022
Published: Mar. 01, 2022

1. Introduction

The increase in global energy demand and the use of non-renewable energy sources, such as fossil fuels, have reduced the availability of these sources, which will not be available once consumed completely [1, 2]. With the depletion of fossil fuels worldwide, alternative energy sources have become important [3]. Renewable energy sources are a suitable alternative because they provide clean energy and reduced strong negative environmental effects, such as air pollution and global warming as well as it being a low-cost source of energy [4-8]. Renewable energy is derived from natural processes that are replenished constantly. In its various forms, renewable energy is derived directly from the sun, wind, rain, tides of the ocean, biomass, and geothermal resources from heat generated deep within the earth [9, 10].

Solar energy is one of the most important forms of renewable energy the radiation from the sun and carries it with them heat and light sources; this energy form can take advantage of the sun in many applications [11-14]. Solar energy can be used for water heating; a solar heater can be used to invest sun irradiation to obtain hot water [15].

As an auxiliary system, solar water heaters are used to reduce the use of conventional fuel by preheating water in industrial and domestic sectors [16]. Nowadays, solar heater is used in many countries worldwide to provide hot water in homes and buildings as well as for industrial applications to generate electricity [17, 18]. Solar energy is one of the important clean sources of energy therefore, conversion methods of this power to useful energy have attracted a great deal of attention in the scientific publishing [19].
A solar heater generally consists of glass-covered box encompassing painted steel tubes, through which water is heated as it circulates by thermo-gravity in the hot water tank [18, 20]. The surface that absorbs solar energy is a major component of the solar heater and is coated with different absorbent materials. Solar energy is easily obtained using a surface coated with a thin layer of black paint [21]. Nanomaterials have also found applications in solar cells [22] as well as many other applications such as photosensors [23], and photocatalyst [24], …etc. This is because of a very important property of nanomaterials which is their very high surface-to- volume ratio.

Different nanomaterials, such as carbon nanotube (CNT) [21, 24] and carbon nanoparticles in NiO, ZnO, and SiO_2 matrices [25], are used to coat solar water heaters. The use of CNPs increases the absorption efficiency of solar collectors. CNPs have drawn considerable interest over the last years due to their high chemical stability, conductivity, and broadband optical absorbance [26, 27]. The development of new materials for solar absorbers remains a challenge. Researchers aim to obtain coatings with a higher coefficient of absorption of solar energy at the lowest production cost.

In the current work, CNPs were prepared by sonication. CNPs-based coating was tested and easily applied to investigate its optical properties and evaluate its thermal performance.

2. Experimental work

2.1. Materials and equipment

Carbon black, ethanol with purity of 99.9%, silicone glue (R.T.V, made in IRI). and temperature sensor (Arduino, China) were used. Optical absorption and reflectance were investigated using UV–Vis. spectrophotometer (ShimadzuUv-1800). The surface morphology of the prepared samples was investigated with a Scanning Electron Microscope (SEM) (Nano Nova 450). Ultrasonicator (type TF-1000) was used to prepare CNPs.

2.2. Preparation of carbon nanoparticles (CNPs)

Carbon nanoparticles were prepared through sonication by adding 5 g of carbon black powder to 60 mL of ethanol. The mixture was placed in a sonicator for 30 min. at room temperature. After that, it was left for 24 h until ethanol evaporated and leaving the CNPs.

2.3. Coating

A 10 g of silicon glue was mixed with 0.05 g of carbon black and the same ratio of CNPs was added to silicon glue to produce a homogeneous paint. The components were manually mixed and used to paint the hot water tank and condenser with a brush. Ddifferent ratios of 0.025, 0.2, 0.05, and 0.1 were used to prepare CB/silicon glue and CNPs/silicon glue films. An experiment was conducted on two solar water heaters filled with water and fitted with a thermometer to compare the thermal performance. The temperature was monitored for 1 month.

Figure 1: Photograph of the designed solar water heater.

2.4. Solar water heating system (SWHS)

The experimental setup is shown in Fig. 1. The system consisted of two identical simple SWHSs, where each was made of a condenser and a storage tank. The condenser was made from a copper tube with a diameter of 1. 5 cm and a length of 2.5 m. The cylindrical storage tank was made of galvanized iron and had a height of 32 cm and a base diameter of 20 cm. The components were placed in a wooden box and covered with a 5 mm-thick glass plate. The collectors were thermally insulated at the back by glass wool to reduce heat loss. The first system (T1) was painted with carbon black paint, and the other system (T2) was painted with CNPs paint. The two experimental systems were mounted on a building rooftop in the city of Basrah (30° 30’ 03” North, 47° 48’ 59” East). They were oriented to face the south direction with a tilt angle of around 45° with the horizon.

3. Results and discussion

3.1. Optical Properties

Fig. 2 shows the UV–Vis. absorbance spectra for the prepared CB/silicon glue and CNPs/silicon glue films with different ratios (0.025, 0.2, 0.05, and 0.1) deposited on glass substrates.

An absorbance peak was found at 320 nm in the spectra of the prepared samples which is around the same wavelengths of the peaks of the spectra of CB and CNPs. This is due to the π–π^* transition in the ultraviolet frequency region. The long tail extended into the visible range is because of the n–π^* transition, in contrast to the data obtained by Tan et al.[28]. Moreover, the 0.05 ratio of carbon nanoparticles film had the highest absorbance compared with the same ratio of carbon black.

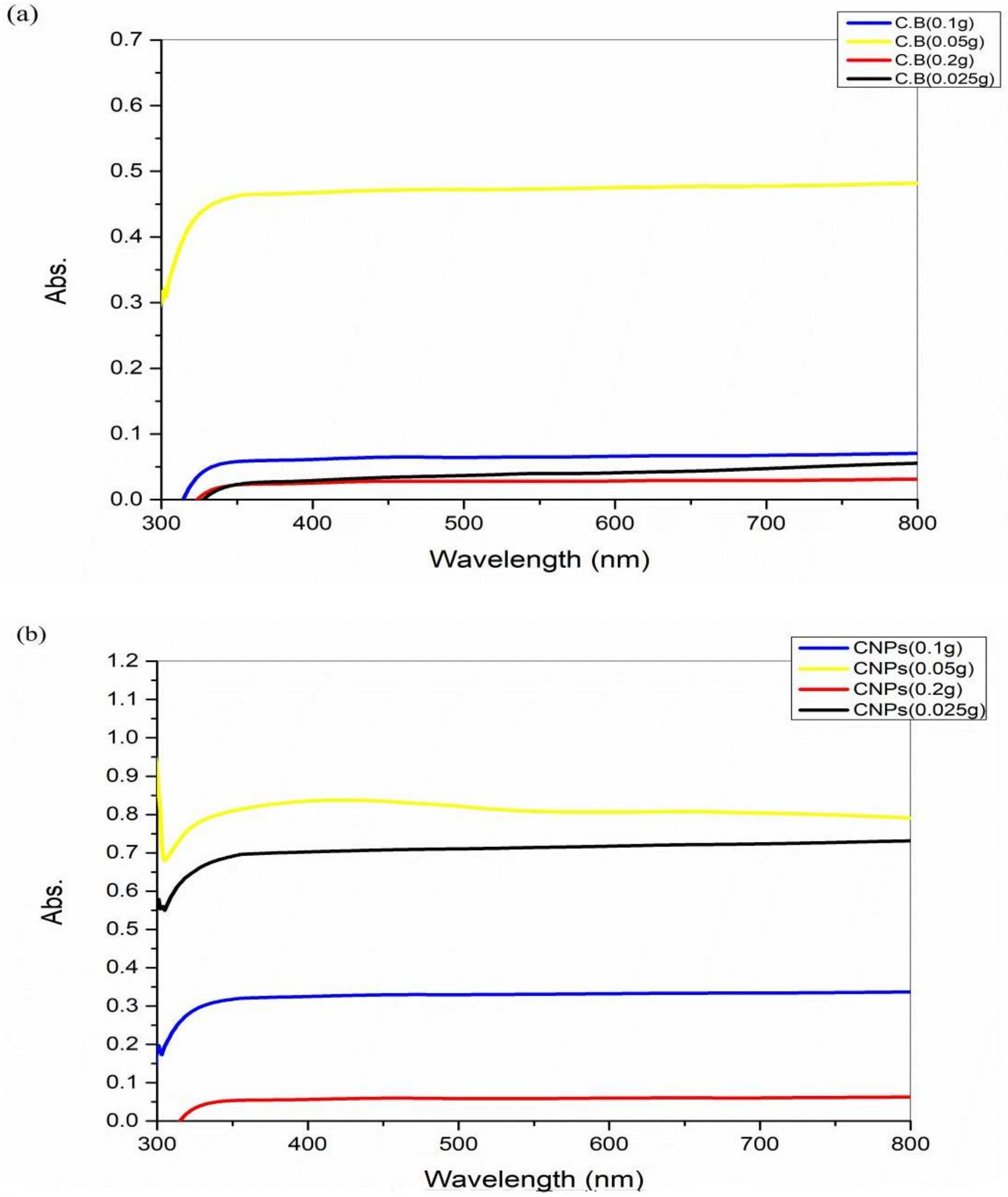

Figure 2: Absorbance spectra of different ratios of: (a) carbon black, and (b) carbon nanoparticles.

Carbon nanoparticles have higher absorbance because the structure and size of each nanoparticle can influence the position of π–π* absorbance [29]. Using carbon nanoparticles as coating paint can enhance the efficiency of the solar water heater.

Fig. 3 shows reflectance spectra of the prepared samples of CB/silicon glue and CNPs/silicon glue films of different ratios (0.025, 0.2, 0.05, and 0.1). The reflectance spectra show two peaks for CB and CNPs at wavelengths of 400 nm and 850 nm, respectively. The first reflectance peak arises because of π-plasmon bands (collective oscillations of π electrons) in the ultraviolet frequency region, and the second reflectance peak is due to π-plasmon bands (collective oscillations of π electrons) in the (IR) frequency region, leading to tall-lived electronic oscillations. The reflectance for CB/silicon glue films of the 0.05 ratio was 0.15% at the wavelength of 400 nm and 0.23% at the wavelength of 850 nm.

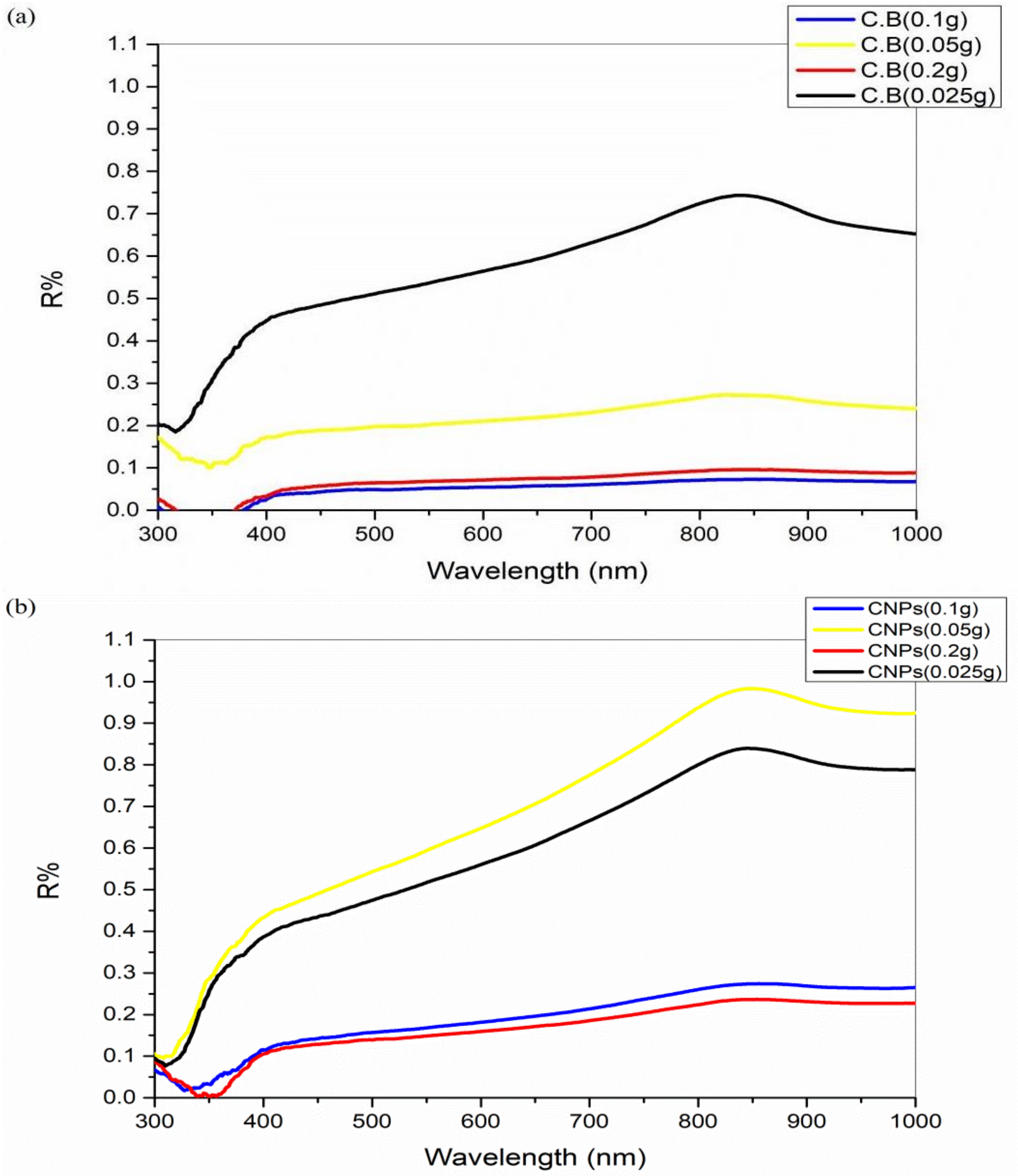

***Figure 3: Reflectance spectra of different ratios of: (a) carbon black, and (b) carbon nanoparticles with silicon glue*.**

While the reflectance of CNPs at the same ratio were 0.45% and 0.99% at the same wavelengths, respectively. However, the reflectance value for all the prepared samples was less than 1% making them suitable to coat solar heater to obtain high efficiency.

3.2. Surface morphology

Fig. 4 shows the FESEM images and histogram plot of the particle size distribution of CB/silicon glue film and CNPs/silicon glue film. The FESEM image of CB/silicon glue in Fig. 4a show white individual particles of a nearly spherical shape with size ranging from (100-400) nm. Comparing with the FESEM image in Fig. 4b, CNPs/silicon glue films have smaller particles size. Moreover, CNPs are homogeneous and spherical, with particle size ranging from (10 -100) nm.

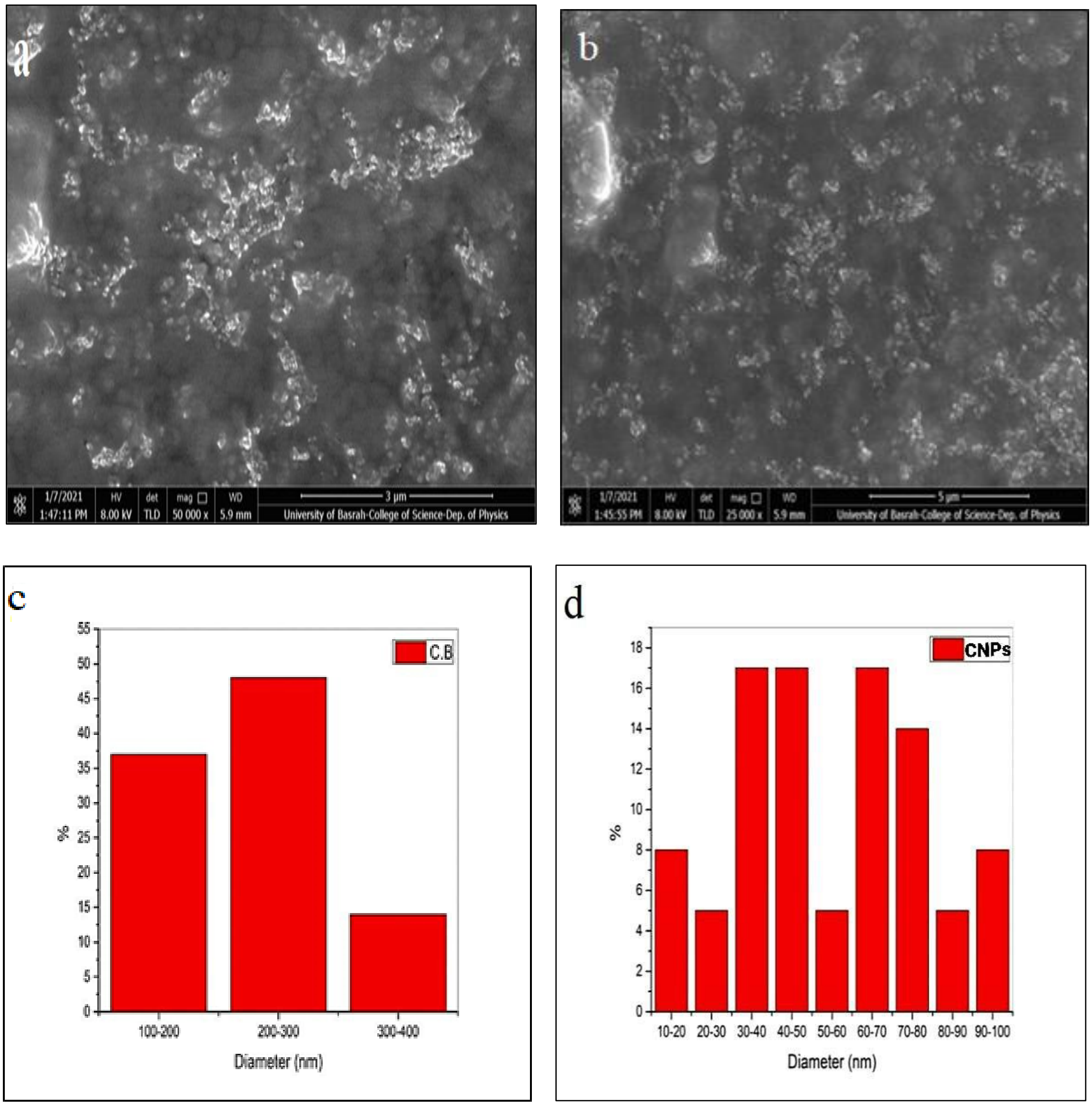

Figure 4: FESEM of: (a) CB/silicon glue film and (b) CNPs/silicon glue film. Particle size distribution of: (c) CB and (d) CNPs.

3.3. SWHS performance

Fig. 5 shows the change of temperature of the water stored in the heater and the water in the cylinder with time for uncoated heater. The temperature is low in the first hours of the morning and gradually increases reaching a maximum value at the hour 14:00; after which, it gradually decreases in the last hours of the day due to the influence of the sun's ray and its angle of incidence. This finding could be due to the fall of the sun's ray in the early hours of the morning on the solar heater at a certain angle and that most of these rays are reflected away from the heater, while the other part is absorbed by the heater and so heats the water to a certain temperature.

At midday, the sun's rays fall perpendicular on the solar heater, thereby increasing the water temperature. In the late hours of the day, solar radiation begins to decrease, leading to a decrease in the temperature of the water. The highest temperature recorded at 14:00 was 46 °C, while the temperature of the water in the cylinder at the same time was 23 °C. The difference is due to the solar heater, which slightly increases the temperature of the water inside it because it works without coating.

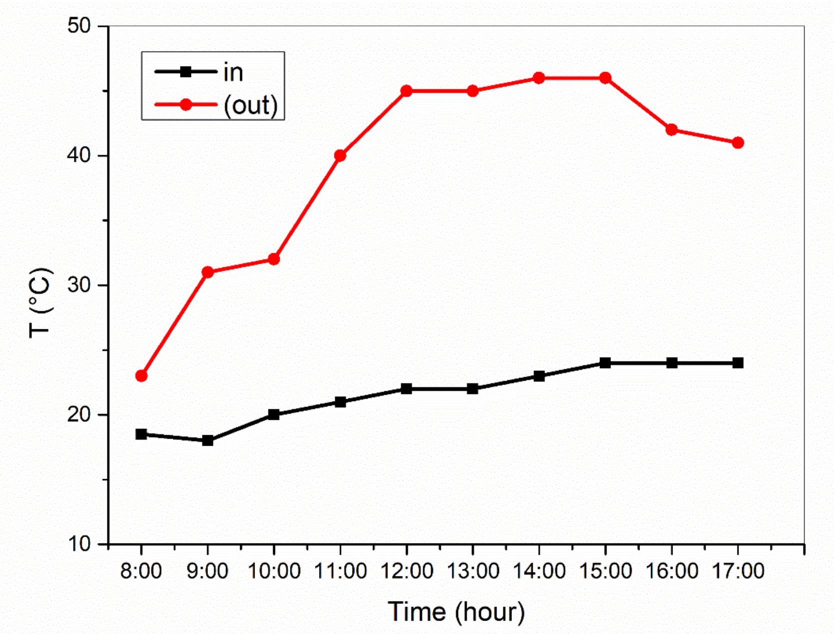

Figure 5: Temperature change during the day hours of the two systems without coating measured at 02.02.2021.

Fig. 6 shows the satisfactory thermal performance of the two heaters. T1 heater recorded a temperature of 65.25°C and T2 heater recorded 69.94 °C at exactly 13:00 in the middle of the day. The performance of the two heaters began to increase from 8:00 until it reached the maximum value (72°C for T1 and 75°C for T2) at 15:00. The figure shows that T2 heater exhibits superior performance. The two heaters were operated under the same conditions and received the same amount of radiation throughout the day. The properties of CNPs characterized by small particle size increase the surface area, thereby increasing their effectiveness for absorbing solar energy radiation. After 15:00, the T1 heater has superior performance because nanomaterials have a large surface area, which increases heat loss in the absence of solar radiation. The solar water heater with the CNPs new paint exhibited better thermal performance than that with carbon black paint, with an average increase in water temperature of 4 °C.

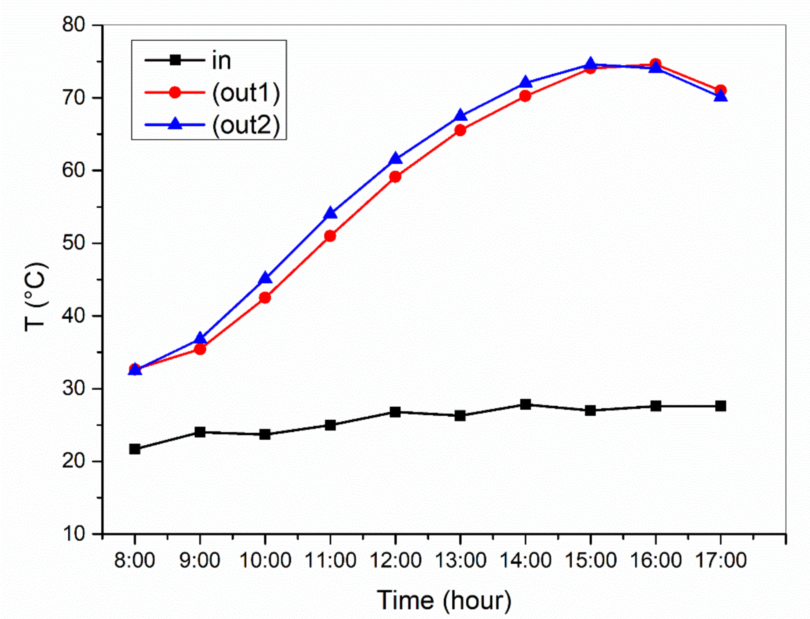

Figure 6: Temperature change during the day hours with coating measured at 15.02.2021.

3.4. Thermal efficiency

Thermal efficiency of the fabricated solar water heater was calculated at some specified hours during the day using Eq. (1) [30]:

$$\eta = m \cdot C_p \, (t_2 - t_1) / I \cdot A_c \qquad (1)$$

where m is the mass of water in kg (which was 10Kg), C_P is the specific heat of water = 4186 J/kg.°C, t_2 is outlet water temperature in °C, t_1 is inlet water temperature in °C, I is the intensity of the incident solar radiation in W.h/m^2, which was previously calculated in the Solar Energy Laboratory at the College of Education-Department of Physics with a solar integrator device, and A_c is the surface area of the collector in m^2.

The surface area of the collector was calculated using Eq. (2) [31]:

$$A = 2 \cdot \pi \cdot r \cdot h + 2\pi \cdot r^2 \qquad (2)$$

where r is the radius of the cylinder in m, and h is the height of the cylinder in m.

Table 1 summarize the calculated thermal efficiency of the fabricated solar heaters T1 and T2 for 10 days, and for specific hours.
The table demonstrate that the thermal efficiency of the designed solar water heater painted with CNP-based paint was better than that of the solar water heater painted with CB. The reason of the different in the thermal efficiency could be due to increase of light absorption of CNPs.

Table 1: The calculated thermal efficiency of the fabricated solar heaters T1 and T2 for 10 days, and for specific hours.

Type of solar water heater	Time	Date	t_1 (°C)	t_2 (°C)	I (W.h/m^2)	η %
The heater coated by CB	13:00	15-02-2021	26.3	65.56	3579	68
	11:00	19-02-2021	19	44.31	2859	55
	13:00	21-02-2021	21	63.56	4900	54
	12:00	22-02-2021	20.1	58.38	3445	69
	12:00	26-02-2021	20	56.886	3209	72
	13:00	6-03-2021	20	63.81	4722	58
	12:00	7-03-2021	20.4	57.94	3635	64
	11:00	13-03-2021	21	46.31	2775	57
	11:00	14-03-2021	22	49.19	2699	63
	11:00	15-03-2021	22.5	51.38	2693	67
The heater coated by CNPs	13:00	15-02-2021	26.3	67.50	3579	72
	11:00	19-02-2021	19	48.56	2859	64
	13:00	21-02-2021	21	67.19	4900	59
	12:00	22-02-2021	20.1	61.44	3445	75
	12:00	26-02-2021	20	60.06	3209	78
	13:00	6-03-2021	20	67.12	4722	62
	12:00	7-03-2021	20.4	62.88	3635	73
	11:00	13-03-2021	21	51.31	2775	68
	14:00	14-03-2021	22	54.69	2699	76
	11:00	15-03-2021	22.5	55.75	2693	77

4. Conclusions

Carbon nanoparticles were prepared using ultrasound waves because this method is easy to conduct, economical, and inexpensive. Moreover, this method can be used for large-scale production of CNPs within a short period of time. When CNPs are distributed in the solution, a smooth surface is obtained, in which the particles are homogeneously distributed and has good nano volume. The solar water heater with carbon nanoparticles coating collected thermal energy more efficiently than the heater coated with carbon black paint. The results of the outdoor experimental study show that the nano-coating produced hotter water.

Acknowledgements

The authors would like to express our appreciation to the University of Basrah, College of Science, Department of Physics, for allowing us to utilize their lab to complete this study. We appreciate their cooperation.

Conflict of interest

The authors declare that they have no conflict of interest.

References

1. Hamdan M. and Sarsour M., *Effect of nanoparticles on the performance of solar flat plate collectors.* Journal of Ecological Engineering, 2018. **19**(2): pp. 1-7.
2. Güney T., *Renewable energy, non-renewable energy and sustainable development.* International Journal of Sustainable Development World Ecology, 2019. **26**(5): pp. 389-397.
3. Gielen D., Boshell F., Saygin D., Bazilian M.D., Wagner N., and Gorini R., *The role of renewable energy in the global energy transformation.* Energy Strategy Reviews, 2019. **24**: pp. 38-50.
4. Walsh M. and Lin W., *A parametric study on the thermal performance of unglazed solar water collectors with their colorbond steel absorber plates also used as roofs.* International Journal of Green Energy, 2015. **12**(12): pp. 1309-1322.
5. Ram M., Bogdanov D., Aghahosseini A., Oyewo S., Gulagi A., Child M., Fell H.-J., and Breyer C., *Global energy system based on 100% renewable energy—power sector.* Lappeenranta University of Technology Energy Watch Group: Lappeenranta, Finland, 2017: pp. 1-26.
6. Twidell J., *Renewable energy resources*. 2021: Routledge.
7. Roespinoedji D., *Experimenting the long-haul association between components of consuming renewable energy: ARDL method with special reference to Malaysia.* International Journal of Energy Economics and Policy, 2019. **9**(6): pp. 453-460.
8. Abdulelah H., Ali B., Mahdi M., Hassan J., Al-Taay H., and Jennings P., *Fabrication and characterization of nanowalls CdS/dye sensitized solar cells.* Physica E: Low-dimensional Systems and Nanostructures, 2017. **90**: pp. 104-108.
9. Solangi Y.A., Longsheng C., Shah S.A.A., Alsanad A., Ahmad M., Akbar M.A., Gumaei A., and Ali S., *Analyzing renewable energy sources of a developing country for sustainable development: an integrated fuzzy based-decision methodology.* Processes, 2020. **8**(7): pp. 1-21.
10. Avtar R., Sahu N., Aggarwal A.K., Chakraborty S., Kharrazi A., Yunus A.P., Dou J., and Kurniawan T.A., *Exploring renewable energy resources using remote sensing and GIS—A review.* Resources, 2019. **8**(3): pp. 1-23.
11. Çobanoğlu N., Karadeniz Z.H., and Turgut A., *Carbon-based Nanofluid Applications in Solar Thermal Energy.* E3S Web of Conferences, 2019. **111**: pp. 1-6.

12. Gong J., Li C., and Wasielewski M.R., *Advances in solar energy conversion.* Chemical Society Reviews, 2019. **48**(7): pp. 1862-1864.
13. Adelakun N.O. and Olanipekun B.A., *A review of solar energy.* Journal of Multidisciplinary Engineering Science and Technology 2019. **6**(12): pp. 11344-11347.
14. Kabir E., Kumar P., Kumar S., Adelodun A.A., and Kim K.-H., *Solar energy: Potential and future prospects.* Renewable Sustainable Energy Reviews, 2018. **82**: pp. 894-900.
15. Kalogirou S.A., *Seawater desalination using renewable energy sources.* Progress in Energy Combustion Science, 2005. **31**(3): pp. 242-281.
16. Vengadesan E. and Senthil R., *A review on recent development of thermal performance enhancement methods of flat plate solar water heater.* Solar Energy, 2020. **206**: pp. 935-961.
17. Jahangiri M., Alidadi Shamsabadi A., and Saghaei H., *Comprehensive evaluation of using solar water heater on a household scale in Canada.* Journal of Renewable Energy Environment, 2018. **5**(1): pp. 35-42.
18. Nshimyumuremyi E. and Junqi W., *Thermal efficiency and cost analysis of solar water heater made in Rwanda.* Energy exploration and exploitation, 2019. **37**(3): pp. 1147-1161.
19. Abdulelah H., Ali B., Mahdi M., Abdullah A.Q., Hassan J., Al-Taay H., and Jennings P., *Fabrication and characterization of porous CdS/dye sensitized solar cells.* J. Sol. Energy, 2016. **2016**: pp. 1-7.
20. Alayi R., Khalilpoor N., Heshmati S., Najafi A., and Issakhov A., *Thermal and environmental analysis solar water heater system for residential buildings.* International Journal of Photoenergy, 2021. **2021**: pp. 1-9.
21. Gautam A., Chamoli S., Kumar A., and Singh S., *A review on technical improvements, economic feasibility and world scenario of solar water heating system.* Renewable Sustainable Energy Reviews, 2017. **68**: pp. 541-562.
22. Mahdi M., Abdul-Hameed A., Ali B., and Al-Taay H., *Fabrication of SiNWs/PEDOT: PSS Heterojunction Solar Cells.* Iranian Journal of Materials Science and Engineering, 2020. **17**(1): pp. 69-76.
23. Bashkany Z., Abbas I.K., Mahdi M., Al-Taay H., and Jennings P., *A self-powered heterojunction photodetector based on a PbS nanostructure grown on porous silicon substrate.* Silicon, 2018. **10**(2): pp. 403-411.
24. Kadhim M., Mahdi M., Hassan J., and Al-Asadi A.S., *Photocatalytic activity and photoelectrochemical properties of Ag/ZnO core/shell nanorods under low-intensity white light irradiation.* Nanotechnology, 2021. **32**(19): pp. 195706.
25. AlShamaileh E., *Testing of a new solar coating for solar water heating applications.* Solar Energy, 2010. **84**(9): pp. 1637-1643.
26. Maddigpu P.R., Sawant B., Wanjari S., Goel M., Vione D., Dhodapkar R.S., and Rayalu S., *Carbon nanoparticles for solar disinfection of water.* Journal of Hazardous Materials, 2018. **343**: pp. 157-165.
27. Li M., Chen T., Gooding J.J., and Liu J., *Review of carbon and graphene quantum dots for sensing.* ACS Sensors, 2019. **4**(7): pp. 1732-1748.
28. Tan Z., Chihara H., Koike C., Abe H., Kaneko K., Sato K., and Ohara S., *Interstellar analogs from defective carbon nanostructures account for interstellar extinction.* The Astronomical Journal, 2010. **140**(5): pp. 1456-1461.
29. Soares M.C., Viana M.M., Schaefer Z.L., Gangoli V.S., Cheng Y., Caliman V., Wong M.S., and Silva G.G., *Surface modification of carbon black nanoparticles by dodecylamine: thermal stability and phase transfer in brine medium.* Carbon, 2014. **72**: pp. 287-295.

30. Manoram R., Moorthy R.S., and Ragunathan R., *Investigation on influence of dimpled surfaces on heat transfer enhancement and friction factor in solar water heater*. Journal of Thermal Analysis and Calorimetry, 2021. **145**(2): pp. 541-558.
31. Ochkov V.F. and Bogomolova E.P., *Teaching mathematics with mathematical software*. Journal of Humanistic Mathematics, 2015. **5**(1): pp. 265-285.

دراسة تأثير جسيمات الكربون النانوية على كفاءة اداء سخان المياه الشمسي

وسن لؤي السالم[1], جاسم مهدي الاسدي[2], مازن عوني مهدي[3]
[1و2]قسم الفيزياء , كلية التربية للعلوم الصرفة , جامعة البصرة , البصرة , العراق
[3]قسم الفيزياء , كلية العلوم , جامعة البصرة , البصرة , العراق

الخلاصة

حضرت جزيئات الكربون النانوية باستعمال تقنية الموجات فوق الصوتية لتهشيم مسحوق الكربون الاسود. تم دراسة التشكل السطحي للكربون الاسود (CB) وجسيمات الكربون النانوية (CNPs) المحضرة باستعمال المجهر الإلكتروني الماسح (SEM). يتراوح حجم الجسيمات من 100 نانومتر إلى 400 نانومتر لـ CB ومن 10 نانومتر إلى 100 نانومتر لـجزئيات الكربون النانوية المحضرة. خلطت جزئيات الكربون النانوية المحضرة وكذلك مسحوق الكاربون (كلا على حده) مع غراء السيليكون وبنسب مختلفة هي 0.025 و 0.2 و 0.05 و 0.1 لتكوين اغشية. تم فحص الخواص البصرية للأغشية المحضرة من خلال تحليلات الانعكاس والامتصاص الضوئي. تم تحديد نسبة 0.05غرام من جزئيات الكربون النانوية المحضرة وكذلك مسحوق الكاربون هي الأفضل للطلاء الشمسي نظرًا لكفاءتها العالية في تصنيع سخان المياه الشمسي ثم يتم إضافتها بعد ذلك إلى غراء السيليكون. في الواقع ، تم جدولة درجة حرارة الماء البارد ودرجة حرارة الماء الساخن في خزان التخزين على أساس كل ساعة بمساعدة جهاز Arduino. كما لوحظت درجة حرارة الغلاف الجوي. وقد لوحظ أنه تم الوصول إلى درجة حرارة مخرج الماء حتى 75 درجة مئوية مقارنة بدرجة حرارة الماء الداخل البالغة 23 درجة مئوية للخزان المطبق بالطلاء القائم على CNP.لوحظ ان الخزان الذي تم طلاءه بجزئيات الكربون النانوية المحضرة يعطي درجة حرارة ماء أعلى بمقدار 4 درجات مئوية عن الخزان المطلي بجزئيات الكربون وذلك بعد شهر واحد من الاختبار تحت إشعاع الشمس. بناءً على النتائج ، تظهر أن كفاءة سخان المياه بالطاقة الشمسية تعتمد بشكل كبير على الاختلاف في درجة حرارة الماء عند مدخل ومخرج السخان. عند مقارنة الكفاءة الحرارية لسخان المياه الشمسي المطلي بطلاء CNP بالكفاءة الحرارية لسخان المياه الشمسي المطلي بواسطة CB ، حيث تبلغ كفاءة سخان المياه الشمسي المطلي بـ CNP حوالي 77٪ ولكن سخان المياه الشمسي مطلي مع CB لديه كفاءة 67٪.